COMPDYN 2013
4th ECCOMAS Thematic Conference on
Computational Methods in Structural Dynamics and Earthquake Engineering
M. Papadrakakis, V. Papadopoulos, V. Plevris (eds.)
Kos Island, Greece, 12–14 June 2013

EVALUATING THE POST-EARTHQUAKE ACCESSIBILITY OF HOSPITALS FOR MITIGATION STRATEGY DECISION SUPPORT BY FRAGILITY AND CONNECTIVITY MODELLING

Indranil Kongar[1], Enrica Verrucci[1,2], Tiziana Rossetto[1], and John Bevington[2]

[1]University College London,
Department of Civil, Environmental & Geomatic Engineering, Gower Street, London, WC1E 6LT.
e-mail: {indranil.kongar.10,e.verrucci,t.rossetto}@ucl.ac.uk

[2]ImageCat Ltd.
Centrepoint House, 2 Denmark Road, Guildford, Surrey, GU1 4DA.
e-mail: {ev,jb}@imagecatinc.com

Keywords: Lifelines, Fragility, Connectivity, Earthquake Engineering, Mitigation.

Abstract. *The aim of this paper is to present a trivial proof of concept for analysing the impact of post-earthquake damage to lifelines on indicators of social resilience. The conceptual methodology is demonstrated by carrying out a GIS-based analysis of the impact of damage to highways bridges on accessibility to emergency healthcare facilities in the Santa Clarita suburb ofLos Angeles. A magnitude 6.9 earthquake from the Santa Susana fault zone was used as a scenario event with bridge damage predicted using the HAZUS methodology to calculate exceedance probabilities and uniform random sampling to assign damage states. Moderate damage state was used as the threshold for bridge closure. The system performance was measured as the mean travel time between neighbourhoods and the local hospital, weighted to account for population. The distribution of delay amongst the population has also been derived. The analysis was repeated for three further scenarios to identify the critical node for prioritisation of mitigation works by comparing the impacts with the post-earthquake scenario. The analysis was based on the Los Angeles County disaster route network with straight-line approximations for travel distance on local roads. Results were compared to those obtained using the actual path distance on local roads and this showed that interpretation of the results could vary depending on the measurement method and the decision variable used. Therefore straight-line distance is not a safe approximation. The methodology proposed here will be expanded in the future for a more detailed study assessing the riskfrom damage to multiple lifelines and using a wider range of indicators.*

1 INTRODUCTION

In the emerging philosophy of resilience, focus moves away from vulnerability and emphasises instead the inherent structural capacities of physical systems and the social capital of communities [1]. Therefore resilience can be classified as having a 'hard' component, associated to land-use and to urban development and a 'soft' component, referring to communities and their social-capital. As represented in the framework of resilience proposed by Verrucci [2], lifelines are at the intersection between these two components. Lifelines are socio-technical systems whose efficiency has direct impact on the ability of the community to perform both routine and emergency response activities. This lifeline efficiency is particularly vulnerable to the impact of natural hazards such as earthquakes since the structural components of lifeline systems are vulnerable to ground shaking and ground displacements. Damage to lifelines can be caused directly due to ground motion or indirectly due to disruption caused by damage to other associated lifelines. This has two impacts, firstly the cost associated with repair or reconstruction and secondly the impact on people, businesses and emergency response activities due to service interruption. Lifeline damage therefore has an effect on the functioning of a community and it is important to understand their level of connection, interdependency and inter-linkages with social systems.

Strategies for assessing and mitigating lifelines risk are commonly based on repair costs and system performance. However, lifelines are socio-technical systems and so it is not the system performance itself which matters, but the impact that reductions in performance have on the community, in terms of both routine and emergency operation. Appraisal of disaster mitigation strategies should therefore use decision variables that account for these social impacts on local communities. Previous studies have developed disaster mitigation decision support tools based on lifelines and community impacts but either focus on a single lifeline only or measure impacts qualitatively [3, 4]. The EPICentre group at University College London have recently started a project, in conjunction with ImageCat (Guildford, UK, Long Beach, CA.) and the Willis Research Network, which aims to produce a more quantitative and holistic decision support tool. As a first step in this exercise, a simplified proof of concept has been produced to demonstrate the concept and the strategy of the proposed tool using a single lifeline. This case study investigates the impact of highway network damage on emergency healthcare accessibility in the Santa Clarita suburb of Los Angeles with decision variables based on travel time, but does not account for decision-making processes. This paper presents the methodology used in this case study and the results obtained from assessing the impacts of a single scenario event. It goes on to discuss the inference of those results and the role that the selection of decision variable plays in how the results are interpreted.

2 METHODOLOGY

2.1 Data acquisition

An evaluation of the spatial connectivity and interdependency of the highway system and health care facilities in Santa Clarita, Los Angeles, has been performed by means of GIS spatial analysis. Spatial overlay, proximity and network analyses have been applied. The study required the acquisition of data on the spatial distribution of the highways network and healthcare facilities as well as the identification of preferred routes between neighbourhoods and healthcare facilities, defined by the shortest travel time. The study has required the acquisition, cleansing and enhancement of several spatial datasets. For data rich case studies, like Santa Clarita, spatial data information were easily obtainable and so several data sources have been investigated. When potentially useful datasets were available from more than one

source, the most recent and up-to date layer was adopted or a final layer was produced based on the spatial comparison of same feature raw layers.

Spatial overlay and proximity analysis have been used in conjunction with each other in order to derive preliminary information about the spatial relationship between the street layer, the healthcare facilities and the neighbourhoods. Network analysis has then been applied to identify the most efficient routes based on travel-time. A simplified road network has been used in the model based on the primary disaster routes designated by the Los Angeles County Department of Public Works (LADPW) [5]. The exclusion of local roads from the analysis is justified since observation shows that the local road network exhibits a high degree of redundancy. Furthermore, where redundancy is high, complete routing analysis becomes computationally intensive.

The road network layer has been obtained by comparing the Census TIGER 2010 [6] road layer with the most recent acquisition of Google Earth satellite imagery [7] and with the disaster route maps produced by LADPW [5]. In some cases the disaster route followed the path of two roads, e.g. a local main road adjacent to an elevated highway. In these cases it was assumed that the disaster route would follow the highway since these have higher traffic carrying capacity. For this proof of concept only ground shaking hazard was considered and so it has been assumed that bridges are the only vulnerable component in the highways network, since roads are more vulnerable to ground deformation. The distribution of highway bridges was extracted as a subset of the California-wide spatial database in the HAZUS software [8] and was compared against the bridge layout of the Caltrans web-GIS platform [9]. The data extracted from HAZUS included structural characteristics allowing for evaluation of fragility. In the cases where bridges were missing from the HAZUS database but included within the Caltrans database, structural typology information has been acquired by querying tabular data published alongside the Caltrans web-GIS platform.

The layer of health facilities has been produced by comparing the subset extracted from HAZUS [8] with tabular data available on the American Hospital Association (AHA) website [10]. The information from the HAZUS layer has been enhanced by adding the number of beds and medical personnel information for each of the medical facilities located in the study area and also entry points to the hospitals. The layers have been integrated into a single geo-spatial database. In this case study, the Santa Clarita suburb was assumed to be a boundary-constrained region with the condition that no flow was possible between Santa Clarita and neighbouring suburbs. This condition consequently meant that the neighbourhoods within Santa Clarita had access to only one hospital.

Based on visual interpretation of the Google Earth satellite image [7], access points to/from the disaster route network have been added to the geo-spatial database to produce the final layer. These include access points between local neighbourhoods and the disaster route network (neighbourhood access points) and access points between the hospitals and the disaster route network (hospital access points).

The Santa Clarita suburb is made up of a number of smaller neighbourhoods and one of the decision variable selected for this analysis accounted for the mean travel time between these neighbourhoods and local hospitals, weighted by neighbourhood population. For the definition of the spatial extent of the neighbourhoods, a simplistic procedure was adopted of visually identifying and manually digitising polygons using Google Earth satellite imagery [7], which were subsequently converted into an ArcGIS shapefile. The layer was validated against the road network, where small neighbourhoods were identified as built-up clusters with a single access main road feeding into a network of local roads. In total 55 neighbourhoods were identified. The complete dataset is shown in Figure 1.

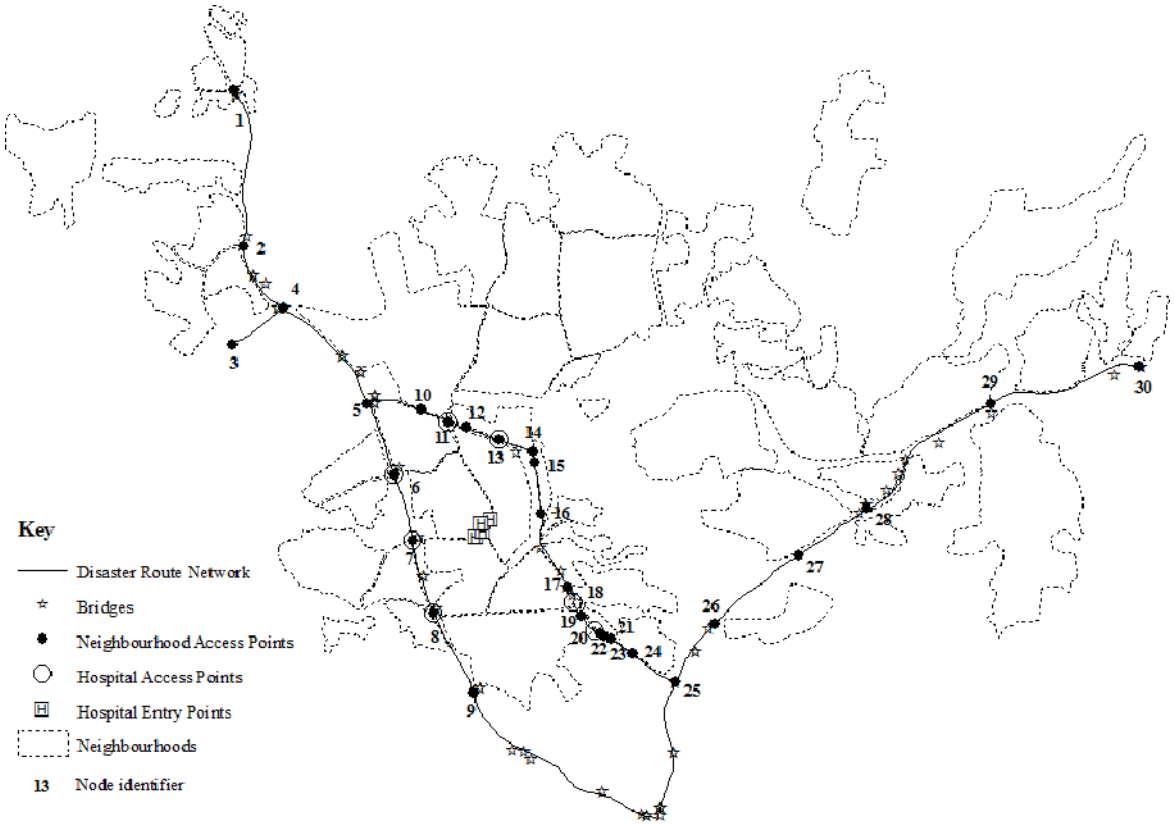

Figure 1: Final dataset of Santa Clarita suburb for GIS analysis including neighbourhood, hospital and highways data

2.2 Hazard

Probabilistic seismic hazard assessment (PSHA) is a common approach to defining hazard for risk assessment exercises. The process identifies the intensity measures (IM) values that will occur with defined return period based on multiple earthquake sources. However this procedure is not appropriate for the risk assessment of lifelines. Firstly, lifelines are spatially distributed and so one cannot assume the same value of IM at all component sites. Secondly, hazard maps display PSHA outputs as fields of IMs but whilst these IMs are predicted to occur at each location within the specified return period, they are not necessarily predicted to occur at the same time. The performance of a system following an earthquake will depend on its fragility and the redundancy it exhibits. System redundancy can only be assessed by understanding the behaviour of components simultaneously in response to a shock. Consequently alternative approaches must be used for spatially distributed systems, which model simultaneous IM values.

It is possible to assess the lifelines risk by selecting a single deterministic event, such an important historic earthquake or a defined maximum credible earthquake from a particular source, then calculating the decision variable for this event. Such an approach has benefits with respect to public engagement of risk but accounts for neither the uncertainty in predicting the location and magnitude of earthquakes, nor the natural variation in strong motion resulting from them. A more robust alternative is to run a Monte Carlo simulation (MCS), using historic earthquake data to generate a stochastic set of deterministic events. These events can be from a single source or from different sources and the MCS approach can account for this locational uncertainty, as well as uncertainty in magnitude, depth and fault characteristics. The decision variable can then be calculated for each event and subsequently

predicted probabilistically from the distribution of these results. This methodology is analogous to the way that the insurance sector estimates building losses for spatially distributed portfolios.

The MCS methodology is proposed for the next stage study, but for this proof of concept a single scenario earthquake has been used for simplicity. Shiraki et al. [11] identified maximum credible earthquakes (MCE) for fifteen fault sources in the Los Angeles area based on an earlier study by Petersen et al. [12]. The scenario selected for the case study was the MCE for the Santa Susana fault zone, the closest fault zone to the Santa Clarita study area. This MCE was attributed with a moment magnitude of 6.9. Other characteristics were unspecified, but not required to calculate peak ground acceleration (PGA) using the selected ground-motion prediction equation (GMPE) developed by Boore & Atkinson [13], which was appropriate for the shallow crustal environment in California. The GMPE also required input values for $V_{s\,30}$, the average shear-wave velocity to 30m depth, which were obtained from the USGS Global $V_{s\,30}$ Map Server [14].

This GMPE includes two residual terms representing inter-event and intra-event variability. The inter-event term is constant at all sites for a single earthquake while the intra-event term varies across all sites. Both residuals are normally distributed with zero mean and specified standard deviations. Thus both residual terms could be estimated by randomly sampling from this distribution. However, the random sampling of the intra-event residual does not account for correlation between IMs at sites close together. A local model for spatial correlation can be applied to resolve this. Whilst this detailed approach is proposed for the next stage of the study, for the proof of concept, this variability was not considered and median values were calculated from the GMPE.

2.3 Lifeline fragility

The damage scenario of a lifeline system identifies the damage state of all components in that system following a single earthquake scenario. The predicted damage state experienced by a lifeline component was related to the IM using fragility functions, which evaluate the exceedance probabilities of pre-defined damage states. To assign a damage state to the component based on these probabilities, a uniformly distributed variable, u, was randomly sampled such that $0 \leq u \leq 1$. The sampled value was then compared to the exceedance probabilities and the damage state was assigned as described in Equation 1. For a fragility function with m damage states, d_0 represents the 'no damage' state and d_m represents the 'complete damage' state. Component i of a lifelines system was assigned to the nth damage state if the condition in Equation 1 was satisfied, where n is an integer between 0 and m, u_i is the sampled random variable for component i and $P_{n,i}$ is the exceedance probability of damage state n for component i at the assessed IM value.

$$P_{n+1,i} < u_i \leq P_{n,i} \tag{1}$$

By repeating for all components, a damage scenario for the system was generated. However, since damage state exceedance is probabilistic, this damage scenario represented just one possible expression of the system response. System performance and subsequent decision variable calculations will change depending on which components are damaged and how severely, as some components will have more importance than others. To account for this uncertainty and reflect the full distribution of possible system responses, a damage scenario MCS should be run for each earthquake. The decision variable could then be calculated for each earthquake and damage scenario pair to produce the exceedance curve. It is proposed that this simulation approach is adopted for the next stage of work, but for this proof of concept, only one damage scenario has been generated for the scenario earthquake.

For the Santa Clarita study, it has been assumed that bridges were the only vulnerable component in the highways network. Damage to roads due to geotechnical effects and displacements were not considered. The bridge data was extracted directly from HAZUS with appropriate structural classification and the HAZUS methodology was used to calculate exceedance probabilities based on local PGA values.

This case study was interested in the performance of emergency services in the immediate aftermath of an earthquake. On this basis it was assumed that damage states of moderate or higher would result in precautionary bridge closure [15]. It may be expected that minor damage could reduce the capacity and hence average speed across a bridge might reduce, but this assumption does not take into account reductions in demand and that the travel times of emergency vehicles are likely to be less affected by such changes. Therefore, it was assumed that a minor damage state has no impact on travel time.

For the assessment of the highways system performance, the highways network was modelled as a graph made up of links (roads) and nodes (junctions). The nodes coincided with either neighbourhood access points or hospital access points or junctions between disaster routes. Bridges were attributed to either a node (e.g. a grade-separated junction) or a link (e.g. an overpass without connection to another link). It was assumed that bridge failure at a node would cause failure of that node and all links connected to that node and bridge failure at a link would cause failure of that link. In some cases, more than one bridge was attributed to a link, in which case failure of at least one bridge would result in link failure. From the identification of failed links and nodes, a post-earthquake highways network was generated.

2.4 Spatial analysis

The calculation of travel time between a neighbourhood and the hospital consisted of three parts. Firstly, the travel time between the neighbourhood and a neighbourhood access point on the disaster route network; secondly, the travel time along the disaster route network and finally, the travel time between a hospital access point on the disaster route network and the hospital itself. To calculate the travel time between the neighbourhoods and the disaster route network, the point (straight-line) distance between the neighbourhood polygon centroid and the nearest neighbourhood access point was measured in ArcGIS. To ensure this scenario was realistic, the assigned access points were checked against a local street map to ensure that they were accessible from the neighbourhood. Where this was not the case, the nearest access points were re-assigned manually and re-measured in ArcGIS. An average speed of 50km/h was assumed for this section. This conservative estimate accounts for delays at intersections and due to congestion. It was then assumed that a vehicle will leave the disaster route network at the closest hospital access point. The disaster route network in this area consisted of two types of road. Most of the network is made up of highways (Interstate 5 and State Route 14), along which an average speed of 130km/h was assumed. A small section of the disaster route network is made up of local main roads (Magic Mountain Parkway and Railroad Avenue), along which an average speed of 80km/h was assumed. Finally between the disaster route network and the hospital, an average speed of 50km/h was assumed since this section returned to the local street network. The hospital had four entry points and point distance was used to measure the distance between the hospital access point on the disaster route network and the nearest entry point.

Two decision variables were evaluated for this study. The first was a mean travel time for all neighbourhoods, weighted according to the residential population of each neighbourhood, from which a mean delay can be inferred. This is designed to ensure that the travel time for more populous areas is attributed greater significance. The population was estimated by examining building occupancy and unit count. The analysis required the acquisition of tax

assessor parcel data, purchased through the LA County GIS portal [16]. This consists of a series of polygons for each taxable unit in a building. This implies that for multi-unit buildings, the parcel data layer presents overlapping polygons of same shape and size.

All buildings are identified by a four-digit use code. The first digit provides information about the occupancy (e.g. "0" identifies residential properties). The second and third digit provide information about the unit count ("01" – single unit; "02" – duplex unit, etc.) for all the residential units, except for condominiums. The last digit helps with the identification of vacant proprieties and condominiums (e.g. "V" – Vacant; "C" – condominiums). The first step of the analysis required the identification of non-vacant residential units and the creation of a "unit count" field based on the second and third digits of the use code. Since for condominiums the unit count cannot be derived from the use code, a "points-in-polygon" analysis was applied to obtain the exact number of units. For this purpose, the co-ordinates of the centroid of the each condominium polygon were calculated. The co-ordinates were used to create a point layer and to automatically delete the overlapping polygons in the original parcel layer. The spatial correlation of all the points falling into the modified polygon parcel layer automatically creates a second unit count field for the condominiums. The population count was then obtained by multiplying the final unit count by the average occupancy per residential unit, derived from the 2010 Census [17] for each zip code.

The populations of each neighbourhood were assigned weights as set out in Equation 2 and the weighted mean travel time, $\bar{t}$, was calculated using Equation 3, where pop_j is the population of neighbourhood j, w_j is the weight attributed to neighbourhood j in a study area with k neighbourhood and t_j is the travel time from neighbourhood j.

$$w_j = \frac{pop_j}{\sum_{j=1}^{k} pop_j} \tag{2}$$

$$\bar{t} = \sum_{j=1}^{k} w_j \times t_j \tag{3}$$

However whilst the mean can provide a trivial and objective statistic for comparison, the compromise from this simplicity is loss of information on the distribution of delay amongst neighbourhoods, e.g. a similar mean delay can result from a few people experiencing a large delay or many people experiencing a short delay. To account for the distribution, the second decision variable measured the number of people experiencing delays greater than a series threshold values using the neighbourhood population estimates. The thresholds ranged from 0%-100% with 10% intervals and the variable was evaluated cumulatively. This variable provides more information than just the mean but subsequently requires more subjective interpretation.

3 ANALYSIS AND DISCUSSION

The mean travel time analysis has been carried out for two scenarios, a baseline scenario with a functioning highways network and a post-earthquake scenario with the highways network modified following fragility analysis. The scenario earthquake used was the 6.9-magnitude MCE centred at the Santa Susana fault area.

The fragility analysis of the earthquake scenario predicted that four bridges would experience extensive damage, two bridges would experience moderate damage and two bridges would experience minor damage. This would result in the closure of six bridges. Figure 2 shows the locations of the closed bridges and the impact this had on the highways

network in terms of links and nodes. This also represented the highways network that was used for post-earthquake network analysis. Four of the bridge closures occurred at nodes. This resulted in the failure of three nodes (5, 6 and 8) and indirectly the six links that connect to these nodes. The other two bridge closures occurred along links and resulted in the closure of these two links: between nodes 2 and 4 and between nodes 9 and 25. In terms of routing, the closures resulted in the loss of three neighbourhood access points and two hospital access points, although both of the closed hospital access points were co-located with closed neighbourhood access points.

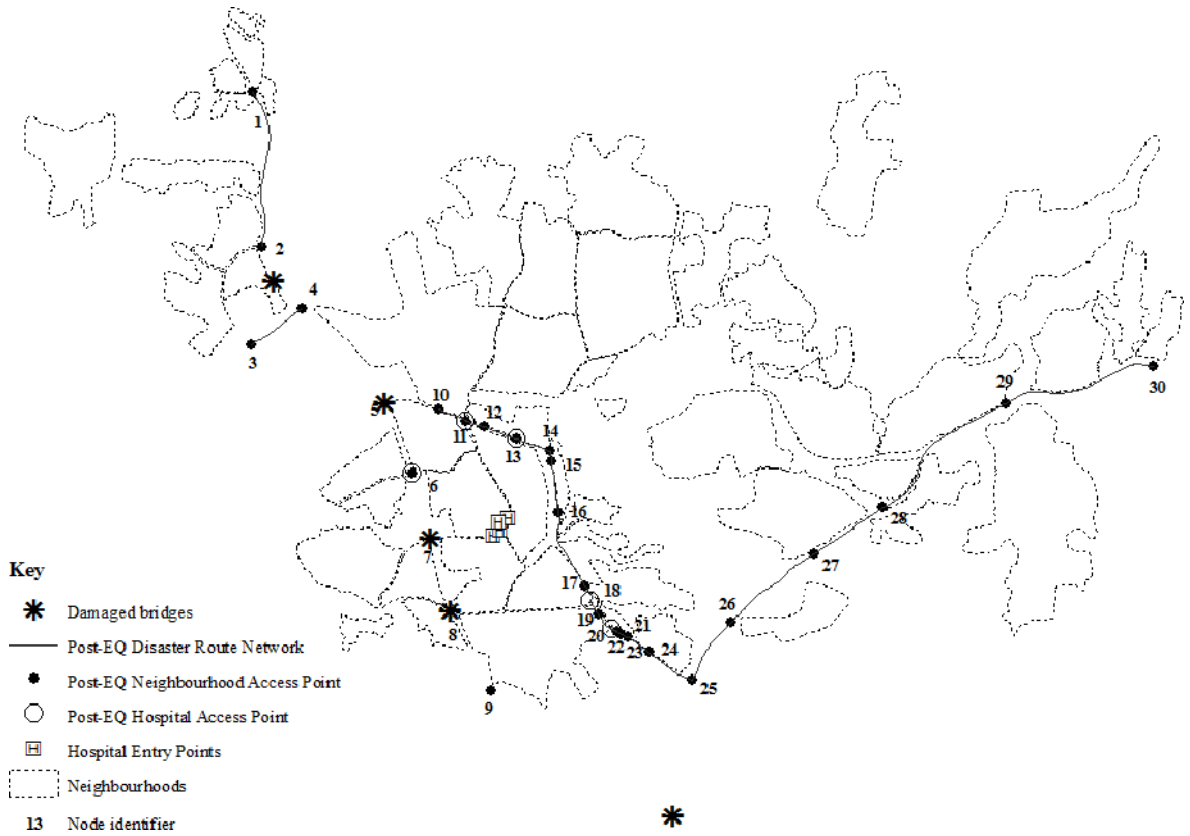

Figure 2: Post-earthquake dataset showing damaged bridges and removal of links from the disaster route network

In the baseline scenario, the weighted mean travel time was calculated at 7m58s. In the post-earthquake scenario, 15 neighbourhoods required re-routing onto the disaster route network, all to the west and northwest of the study area. For the re-routing, it was assumed that a vehicle would travel to the nearest neighbourhood access point that had an unbroken route to a hospital access point, i.e. routes which required vehicles to leave the disaster network at a damaged component and re-join downstream were excluded. Because of redundancy in the local street network, no neighbourhoods became isolated as a result of the predicted bridge damage. For the post-earthquake scenario, the weighted mean travel time was computed as 8m36s. However, because of the approximations and assumptions used in the routing exercise, these absolute travel time values are not in themselves useful. Rather it is the relative performance that is informative and here the earthquake scenario results in a travel time increase of 7.9%. This delay appears small indicating that there is a high degree of resilience in the local disaster route network.

One approach for mitigation planning is to use risk assessment analyses to compare the impact of alternative mitigation strategies. This concept has been demonstrated in this case study by measuring the weighted mean travel time for three further scenarios. In each scenario, one of the failed nodes (5, 7 or 8) was restored to the post-earthquake highways network, simulating the case where the bridge at that node was strengthened prior to the earthquake and therefore did not experience a level of damage requiring necessitating its closure. The fragility analysis was not re-run for these scenarios, which have been designed to identify the most critical node and thus the priority for mitigation interventions. The cases of the two direct link failures were not considered in the sensitivity analysis since neither would improve travel time if restored, due to their location. Table 1 shows the impact on mean travel times in these scenarios. The analysis shows that restoration of node 5 results in the largest reduction in delay. Hence, it is the most critical node and the bridge at node 5 should be prioritised for mitigation. This result was expected from observation since this node is essential to service the neighbourhoods to the northwest of the study area.

Scenario	Weighted mean travel time	% Delay
Baseline	7m58s	-
Post-earthquake	8m36s	7.9
Post-earthquake Node 5 restored	8m17s	3.8
Post-earthquake Node 7 restored	8m28s	6.1
Post-earthquake Node 8 restored	8m33s	7.2

Table 1: Post-earthquake travel time impacts using point distance analysis. The candidate restoration nodes are shown in Figure 2. The % Delay relates to the increase in weighted mean travel time compared to the baseline scenario.

The distribution of the delay amongst the population for each scenario is shown in Figure 3. The results show why the interpretation of this data is more difficult than the mean. The analysis of mean travel time is clear in its identification of the most critical node, albeit at the expense of completeness in terms of information. The distribution is more informative but the results are less clear and more open to subjective interpretation. With the restoration of Node 5, very few people experience delays greater than 50%, and significantly fewer than the other mitigation scenarios. However, in the Node 5 restoration scenario, there are more people who experience an 80% delay than the other two scenarios. Also the Node 7 restoration scenario is clearly the best for minimising the number of people who experience any kind of delay, i.e. total number of people affected. A planner would therefore have to decide which is more important, the total number of people affected or the frequency of large delays only. If the latter, then another decision needs to be made on what the threshold of a large delay should be, i.e. at what point does a delay become unacceptable. This is irrespective of whether delay is presented in percentage or absolute terms. However, Figure 3 also highlights the usefulness of the distribution. In the initial post-earthquake scenario, nearly 35,000 people (approximately one sixth of the total population), experience a delay of over 40%. Also in terms of mean delay, the Node 5 restoration scenario more than halves the delay caused by the earthquake, yet in terms of total number of people affected (delay> 0%), the benefit of restoring Node 5 is not nearly as great.

It is worth noting that, as a decision variable, delay also excludes information. Delay, whether measured in percentage terms or absolutely, does not take into account whether the post-earthquake travel time is actually significant. For example, compare two neighbourhoods, one of which has a baseline travel time of 1 minute and post-earthquake travel time of 6

minutes and another which has a baseline travel time of 10 minutes and a post-earthquake travel time of 15 minutes. Both have the same numerical delay and the former has a much greater percentage delay yet for emergency treatment, the latter neighbourhood has a more significant delay, since its post-earthquake travel time is now quite high. Therefore, it is not that the delay that is important but the actual travel time, which can be compared to a target threshold. One then needs to decide what an acceptable travel time for a vehicle to travel to an emergency medical facility is. It is likely that this will vary from place to place as the acceptable travel time will increase as the extents of the area served by the hospital widen. Where the area is large, the acceptable travel time might also need to be tiered, i.e. for some neighbourhoods a higher travel time is tolerated because of the distance from the hospital. This highlights the importance of including societal and community considerations in infrastructure performance evaluation. Wholly physical system performance metrics, such as delay, only measure vulnerability. It is only by including societal considerations that the emphasis can shift to capacity, as prescribed by the resilience philosophy. This approach was not used in this proof of concept since it requires dialogue with local healthcare providers and planners, but will be considered in the next stage of the study.

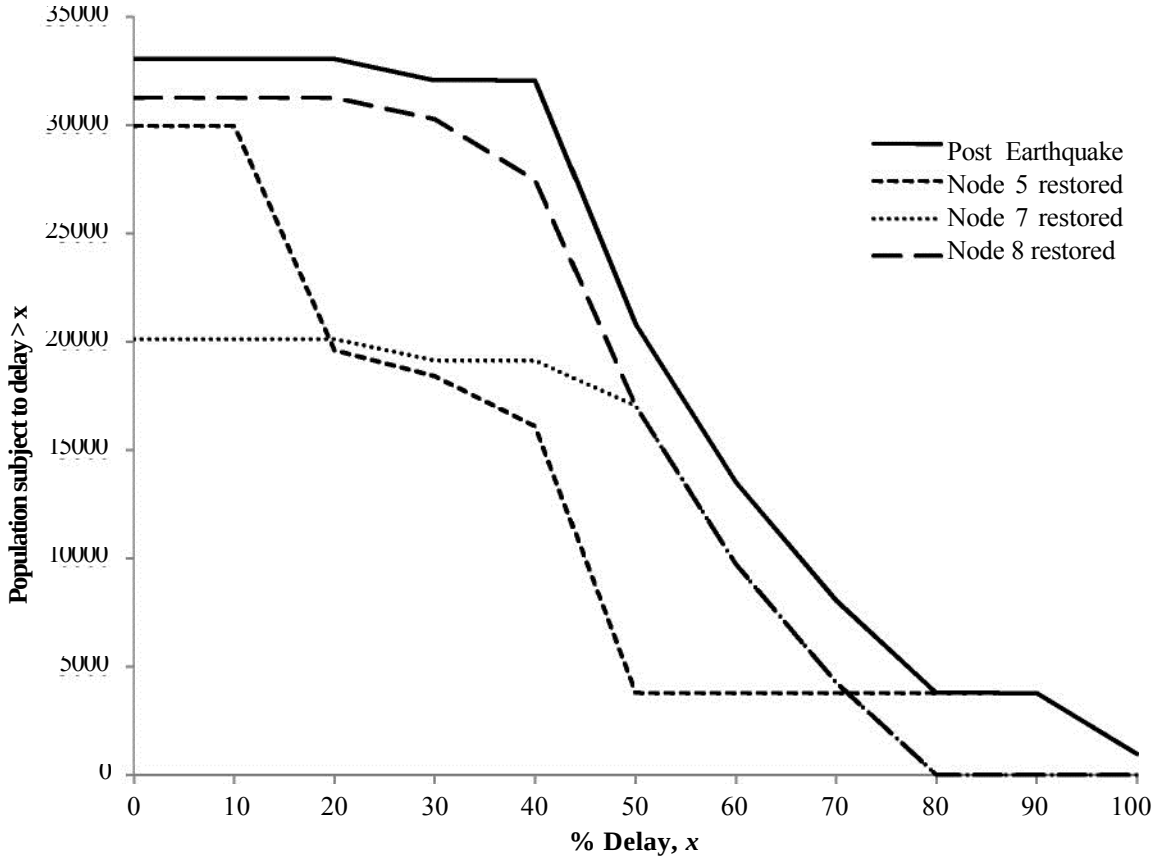

Figure 3: Cumulative distribution of population against the percentage delay in travel time using point distance analysis. The cumulative frequency is measured at 10% intervals.

One of the approximations used in the analysis was the use of point distance between the neighbourhoods and the disaster route network, and also between the hospital and the disaster route network. In most cases road networks are unlikely to follow a straight-line path and so the distance measured is underestimated. The nature and complexity of road networks is such

that the difference between point distance and path distance (measured along roads) can itself vary significantly between neighbourhoods and so the relationship between the two cannot be generalised. The use of point distance could therefore skew the results in certain scenarios where one or more neighbourhoods exhibit a large difference between their point distance and path distance measurements.

As a sensitivity test, the whole analysis, including node restoration was repeated using the actual road distance between neighbourhood centroids and the neighbourhood access points and between the hospital access points and the hospital. This was done by overlaying the shapefile of the final dataset onto a Bing street layout base map embedded within ArcGIS [18] and using the functionality of ArcGIS to trace and measure a path along the local roads, using a heuristic approach for routing based on observed street hierarchy. This heuristic method was only practical for this case study due to the network being small. For a larger network, the local roads would need to be digitised in ArcGIS and the routing analysis undertaken computationally using a shortest-path algorithm. Nevertheless, the heuristic approach provides an approximate indication of how the point distance and path distance methods compare. The new path distance results are shown in Table 2 and Figure 4.

Scenario	Weighted mean travel time	% Delay
Baseline	9m19s	-
Post-earthquake	10m07s	8.6
Post-earthquake Node 5 restored	9m50s	5.5
Post-earthquake Node 7 restored	9m52s	5.8
Post-earthquake Node 8 restored	10m03s	7.8

Table 2: Post-earthquake travel time impacts using path distance.

The comparison shows that the mean delay caused by the earthquake is slightly higher in percentage terms when using the path distance for all post-earthquake scenarios except the Node 7 restoration scenario. The differences are small except for the Node 5 restoration scenario. Since the baseline travel time is higher when using path distance, one might expect the delays to decrease in percentage terms. However this is probably offset since damage to bridges increases the travel time spent on local roads, which is the component of total travel time underestimated by using point distance. Table 2 shows similar values for percentage delay compared to Table 1 and if this method was used for identification of critical node, the result is the same (Node 5), indicating that point distance is a useful approximation. Figure 4 shows that the Node 5 restoration scenario is the worst of the mitigation scenarios for total number of people affected. It also has the highest number of people experiencing delays above 60%. When using the full distribution of information like this, the selection of threshold values for decision making is critical. The results show that depending on the threshold chosen, the two methods, point distance and path distance, would provide different solutions for the identification of critical node. Therefore the validity of using point distance is dependent on the decision variable being used. Since individual networks are unique and complex, there is no way of confirming the validity of using point distance without undertaking full analysis with both distance measurement methods, so there is no actual reduction in computation. Consequently, it is proposed in the next stage of the study to use path distance from the outset.

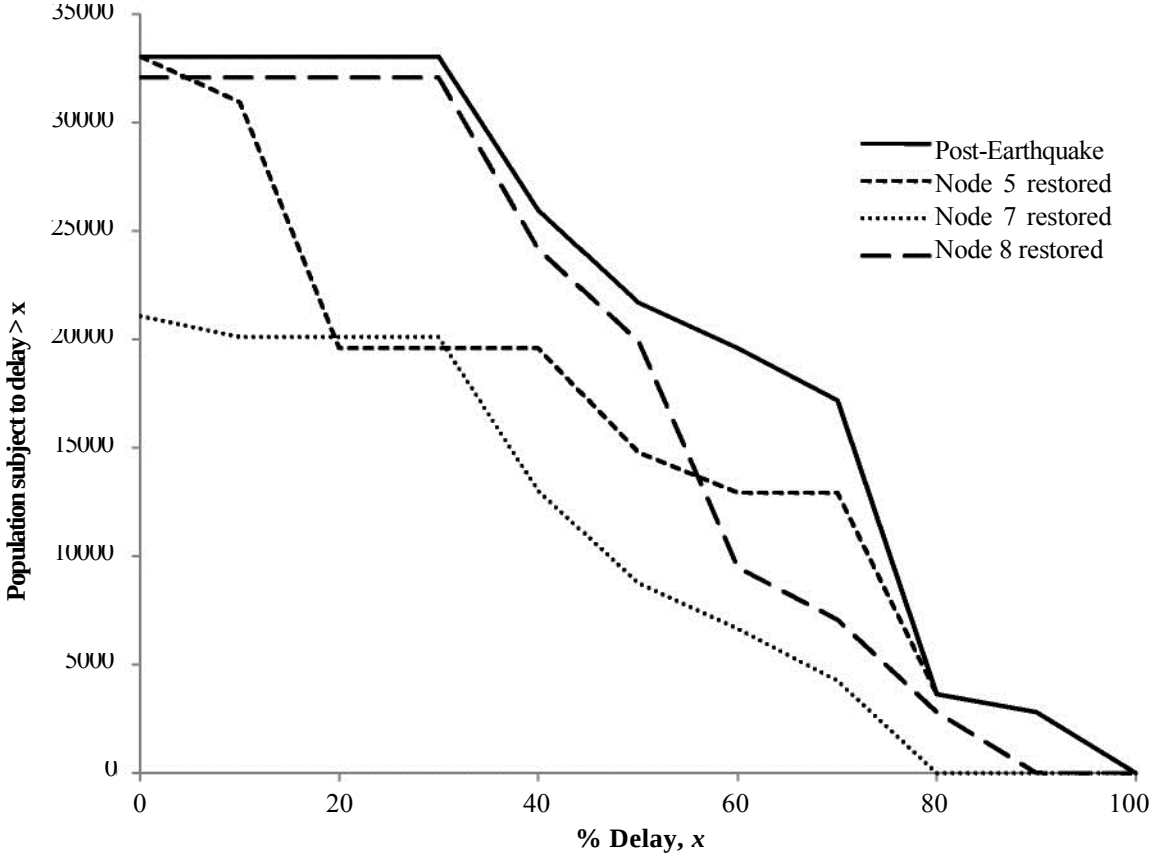

Figure 4: Cumulative distribution of population against the percentage delay in travel time using path distance analysis. The cumulative frequency is measured at 10% intervals.

4 CONCLUSIONS

The analysis described in this paper has demonstrated a simple GIS-based method for assessing highways system performance and the consequent impact on access to healthcare facilities using the Santa Clarita suburb of Los Angeles as a case study. It has also shown how outputs from risk assessment can be used to appraise disaster mitigation strategies. The simplicity of the method allows it to be used and understood by those without expert knowledge in programming and can thus play an important role in making the public and local officials more aware of risk assessment and increasing the perception of risk. Whilst it is possible to undertake more complex analysis using more powerful platforms, a simplified approach is appropriate in certain circumstances such as community engagement and prioritisation of mitigation.

However this case study has been undertaken only as a proof of concept for a larger more detailed study, involving a wider range of lifelines and impacts, and its purpose has been to demonstrate the strategy rather than the detailed methodology, aspects of which will be specific to the case study location. The next stage of the project is to upscale the proof of concept. In particular the methodology described here requires revision to more robustly account for uncertainty. It has already been proposed that Monte Carlo simulation (MCS) should be used to account for uncertainty in hazard and assignment of damage states to components, but these are not the only sources of uncertainty. There is also uncertainty in the selection of GMPE, the inter-event and intra-event variability in GMPE and the relationship between component performance and damage state. One possibility could be to carry out a

MCS for each of these variables too, but that would make the computation prohibitively large. The issue of uncertainty needs to be explored further and is critical in developing a robust tool for interdependent lifelines risk assessment.

Finally, there are also aspirations in the forthcoming stages of the project to investigate a wider range of performance indicators. Current practice in risk assessment focuses on loss estimation and, to a lesser degree, casualties. However, the impacts of an earthquake extend beyond this. The impacts can also be measured in terms of the effect on critical services and the resilience of communities. Building on the work by Verrucci [1], it is proposed to establish a series of key social indicators that can be used to characterise both risk and resilience in relation to lifelines.

REFERENCES

[1] S.C. Moser, *Resilience in the Face of Global Environmental Change*. CARRI Research Report 2. Oak Ridge National Laboratory, US Department of Energy, Tennessee, 2008.

[2] E. Verrucci, *Multi-disciplinary Indicators to Measure and Monitor Earthquake Resilience by using Remote sensing and GIS*. MPhil Report. University College London, London, 2010.

[3] N. Basoz, A.S. Kiremidjian, *Risk Assessment for Highway Transportation Systems*. Blume Report No. 118, Stanford University, California, 1996.

[4] C.A. Bana e Costa, C.S. Oliveira, V. Vieira, Prioritization of bridges and tunnels in earthquake risk mitigation using multicriteria decision analysis: application to Lisbon. *The International Journal ofManagement Science*, **36**, 442-450, 2008.

[5] Los Angeles County Department of Public Works, *Disaster Routes: Los Angeles County Operational Area*. http://dpw.lacounty.gov/dsg/DisasterRoutes (accessed 20 January 2013).

[6] United States Census Bureau (Department of Commerce), *2010 Census TIGER/Line® Shapefiles*. http://www.census.gov/geo/www/tiger/tgrshp2010/tgrshp2010.htm (accessed 20 January 2013).

[7] Google Earth 6.2.2.6613, *Santa Clarita, Los Angeles*. Satellite Image Data Layer. Available through http://www.google.co.uk/intl/en_uk/earth/index.html/ (accessed 20 January 2013).

[8] National Institute of Building Sciences, *HAZUS MR4 Technical Manual*, Washington D.C., 2003.

[9] Calfornia Department of Transport, *Caltrans Earth*. http://earth.dot.ca.gov/ (accessed 29 January 2013).

[10] American Hospital Association, *AHA Health Care Data Viewer*. http://www.ahadataviewer.com/ (accessed 29 January 2013).

[11] N. Shiraki, M. Shinozuka, J.E. Moore, S.E. Chang, H. Kameda, S. Tanaka, System risk curves: probabilistic performance for highway networks subject to earthquake damage. *Journal ofInfrastructure Systems*, **13**, 43-54, 2007.

[12] M.D. Petersen, W.A. Bryant, C.H. Cramer, T. Cao, M. Reichle, A.D. Frankel, J.J Lienkaemper, P.A. McCrory, D.P. Schwartz, *Probabilistic Seismic Hazard Assessment*

for the State of California. Open-File Rep. No. 96-08, California Department of Conservation, Division of Mines and Geology, Sacramento, California, 1996.

[13] D.M. Boore, G.M. Atkinson, Ground-motion prediction equations for the average horizontal component of PGA, PGV and 5%-damped PSA at spectral periods between 0.01s and 10.0s. *Earthquake Spectra*, **24(1)**, 99-138, 2008.

[14] United States Geological Survey, *Global V_S^{30} Map Server*. http://earthquake.usgs.gov/hazards/apps/vs30/ (accessed 30 January 2013).

[15] J.E. Padgett, R. DesRoches, Bridge functionality relationships for improved seismic risk assessment of transportation networks. *Earthquake Spectra*, **23(1)**, 115-130, 2007.

[16] Los Angeles County, *Los Angeles County GIS Data Portal – Assessor Parcels*. http://egis3.lacounty.gov/dataportal/?s=tax+assessor&submit.x=0&submit.y=0&submit=Search (accessed 30 January 2013).

[17] United States Census Bureau (Department of Commerce), *American Fact Finder*. http://factfinder2.census.gov/faces/nav/jsf/pages/searchresults.xhtml?refresh=t/ (accessed 30 January 2013).

[18] ESRI ArcMap 10.0, *Bing Maps Road Layer*. Available through http://www.esri.com/ (accessed 30 January 2013).